PHYSICAL REVIEW E **87**, 041003(R) (2013)

Lagrangian single-particle turbulent statistics through the Hilbert-Huang transform

Yongxiang Huang (黄永祥),[1,*] Luca Biferale,[2] Enrico Calzavarini,[3] Chao Sun (孙超),[4] and Federico Toschi[5]

[1]*Shanghai Institute of Applied Mathematics and Mechanics, Shanghai Key Laboratory of Mechanics in Energy Engineering, Shanghai University, Shanghai 200072, People's Republic of China*

[2]*Department of Physics and INFN, University of Tor Vergata, Via della Ricerca Scientifica 1, I-00133 Roma, Italy*

[3]*Laboratoire de Mécanique de Lille, CNRS/UMR 8107, Université Lille 1, F-59650 Villeneuve d'Ascq, France*

[4]*Physics of Fluids Group, Faculty of Science and Technology, J. M. Burgers Centre for Fluid Dynamics, University of Twente, P.O. Box 217, 7500 AE Enschede, The Netherlands*

[5]*Department of Physics, and Department of Mathematics and Computer Science and J.M. Burgerscentrum, Eindhoven University of Technology, NL-5600 MB Eindhoven, The Netherlands*

(Received 21 December 2012; published 22 April 2013)

The Hilbert-Huang transform is applied to analyze single-particle Lagrangian velocity data from numerical simulations of hydrodynamic turbulence. The velocity trajectory is described in terms of a set of intrinsic mode functions $C_i(t)$ and of their instantaneous frequency $\omega_i(t)$. On the basis of this decomposition we define the ω-conditioned statistical moments of the C_i modes, named q-order Hilbert spectra (HS). We show that such quantities have enhanced scaling properties as compared to traditional Fourier transform- or correlation-based (structure functions) statistical indicators, thus providing better insights into the turbulent energy transfer process. We present clear empirical evidence that the energylike quantity, i.e., the second-order HS, displays a linear scaling in time in the inertial range, as expected from a dimensional analysis. We also measure high-order moment scaling exponents in a direct way, without resorting to the extended self-similarity procedure. This leads to an estimate of the Lagrangian structure function exponents which are consistent with the multifractal prediction in the Lagrangian frame as proposed by Biferale *et al.* [Phys. Rev. Lett. **93**, 064502 (2004)].

DOI: 10.1103/PhysRevE.87.041003 PACS number(s): 47.27.Gs, 02.50.−r, 47.27.Jv, 89.75.Da

The statistical description of a tracer trajectory in turbulent flows still lacks a sound theoretical and phenomenological understanding [1,2]. Presently, analytical results linking the Navier-Stokes equations to the statistics of the velocity increments $v(t+\tau)-v(t)$ along the particle evolution are missing. On the grounds of dimensional arguments, pure scaling laws are expected for time increments larger than the Kolmogorov dissipative time τ_η and smaller than the large-scale typical eddy turnover time $\mathcal{T}_L$. The ratio between the two time scales grows with the Reynolds number as $\mathrm{Re} \propto \mathcal{T}_L/\tau_\eta$. Despite many numerical and experimental attempts [3–7], clear evidence of scaling properties still needs to be detected in the Lagrangian domain even at high Reynolds numbers. Such a fact can be explained by either invoking ultraviolet and infrared effects induced by the two cutoffs τ_η and $\mathcal{T}_L$ or by a real pure breaking of scaling invariance, independently of the Reynolds number [8,9]. Up to now, most of the attention has been paid to the so-called Lagrangian structure functions (LSFs), i.e., moments of velocity increments,

$$S_q(\tau) = \langle |v_j(t+\tau) - v_j(t)|^q \rangle, \tag{1}$$

where, for simplicity, we have assumed isotropy and dropped any possible dependency of the left-hand side on the component of the velocity field. Phenomenological arguments based on a "bridge" relation between Eulerian and Lagrangian statistics [10–16] predict the existence of scaling properties also in the Lagrangian domain $S_q(\tau) \sim \tau^{\zeta_L(q)}$ for $\tau_\eta \ll \tau \ll \mathcal{T}_L$, with $\zeta_L(q)$ being related to the Eulerian scaling exponents $\zeta_E(q)$, defining the scaling properties of velocity increments between two points in the laboratory reference frame. Such a relation has been well verified in the limit of very small time increments, by studying the statistics of flow acceleration [12] or by using relative scaling properties [17], i.e., studying one moment versus another one, a procedure known as extended self-similarity (ESS) [18]. On the other hand, clear evidence of direct scaling properties as a function of τ still needs to be detected (see Refs. [8,9] for two recent papers discussing this problem). As a result, despite the successful comparisons, using ESS, between theoretical predictions for $\zeta_L(q)/\zeta_L(2)$ and numerical and experimental Lagrangian measurements (see Ref. [17]), the absence of a clear scaling range *in the time domain* has cast doubts, on the one hand, on the correctness and accuracy of the present phenomenological models, and, on the other hand, on the fact that SF may not be the suitable statistical indicator to study turbulent flows in the Lagrangian domain [9]. One of the main concerns regards possible nonlocal effects induced by either large-scale and low-frequency modes or by small-scale and high-frequency events that may result in subleading spurious contributions. It is well known, for example, that the temporal evolution of the velocity field along a Lagrangian trajectory in turbulent flows is strongly influenced by the presence of small-scale vortex filaments inducing visible high-frequency oscillations even on the single-particle velocity signal (see Fig. 1 and Ref. [19]). In this Rapid Communication we want to apply a technique, called the Hilbert-Huang transform (HHT), to analyze multiscale and multifrequency signals, which has revealed to be particularly useful in the data analysis of many complex systems [20–25]. HHT has been recently applied to analyze Eulerian turbulent data [26–28], showing an unexpected ability to disentangle multiscale contributions. The main interest in HHT lies in its frequency-amplitude *adaptive* nature, being based on the decomposition of the original signal on a set of *quasieigenmodes*

*yongxianghuang@gmail.com

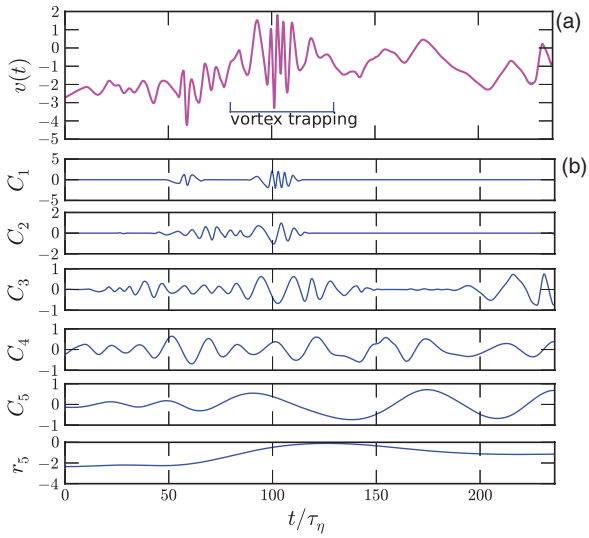

FIG. 1. (Color online) (a) An example of Lagrangian velocity $v(t)$ with a vortex trapping event from the DNS simulation. The data show the multiscale nature of Lagrangian turbulence with different time scales (structures) superimposed on each other. (b) Example of the decomposition of the above trajectory in intrinsic mode functions from empirical mode decomposition. Note that the Lagrangian velocity is separated into different functions with different time scales. The empirical mode decomposition approach reveals the multiscale property of the Lagrangian velocity at a local level.

that are *not defined a priori* [29,30]. The idea is to *not introduce* in the analysis any systematic predefined structures as it always happens using Fourier-based methodologies (e.g., Fourier decomposition or wavelet transforms).

In this Rapid Communication, we apply and generalize the HHT methodology to extract the hierarchy of the Lagrangian scaling exponent $\zeta_L(q)$. The method is applied to the fluid trajectory data obtained from direct numerical simulations (DNSs) at $\mathrm{Re}_\lambda = 400$ (see Fig. 1). We present clear empirical evidence of scaling properties in the usual sense, as a power of the analyzed frequency, also in the Lagrangian domain. We show that the measured Hilbert-based moments $\mathcal{L}_q(\omega)$ display a clear power law in the range $0.01 < \omega\tau_\eta < 0.1$ at least up to the maximum order allowed to be measured by our statistics, $0 \leqslant q \leqslant 4$. The exponents are in good quantitative agreement with the one predicted by using the "bridge relation" based on multifractal phenomenology [12], supporting even more the close relationship between Eulerian and Lagrangian fluctuations at least for what concerns velocity increments in three-dimensional (3D) isotropic and homogeneous turbulence. The data set considered here is composed of Lagrangian velocity trajectories in a homogeneous and isotropic turbulent flow obtained from a 2048^3 ($\mathrm{Re}_\lambda = 400$) DNS simulation (see more details in Ref. [31]). We analyze all the available $\sim 2 \times 10^5$ fluid tracer trajectories, each composed of $N = 4720$ time samplings of $v_j(t)$ (where $j = 1,2,3$ denotes the three velocity components) saved every $0.1\tau_\eta$ time units. Therefore, we can access the time scale from $0.1 < \tau/\tau_\eta < 236$, corresponding to the frequency range $0.004 < \omega\tau_\eta < 10$.

The HHT is a procedure composed of two steps. The first step is the decomposition of the signal into its intrinsic mode functions (IMFs) followed by the Hilbert transform on such modes. In the first step, through a procedure called empirical mode decomposition (EMD), we decompose each velocity time series into the sum

$$v(t) = \sum_{i=1}^{n} C_i(t) + r_n(t), \tag{2}$$

where $C_i(t)$ are the IMFs and $r_n(t)$ is a small residual, an almost constant function characterized by having at most one extreme along the whole trajectory (which will therefore be neglected in the following analysis) [29,30]. In Eq. (2) n may depend on the trajectory, with a maximum value which is linked to its length as $n_{\max} = \log_2(N) \simeq 12$. Given the actual length of our trajectories, with $n \simeq 6$–7, we are typically able to reconstruct the full behaviors (see Fig. 1).

To be an IMF, each $C_i(t)$ must satisfy the following two conditions: (1) The difference between the number of local extrema and the number of zero crossings must be zero or one; and (2) the running mean value of the envelope defined by the local maxima and the envelope defined by the local minima is zero. Indeed, the IMF is an approximation of the so-called monocomponent signal, which possesses a well defined instantaneous frequency [29,32]. The physical meaning of such decomposition is clear: We want to decompose the original trajectory into *quasieigenmodes* with locally homogeneous oscillating properties [29,33]. In the second step, one performs a Hilbert transform for each of the IMFs,

$$\overline{C}_i(t) = \frac{1}{\pi}\mathrm{P}\int \frac{C_i(t')}{t - t'}dt', \tag{3}$$

where P stands for the Cauchy principal value. This allows to retrieve the *instantaneous* frequency associated to each C_i via

$$\omega_i(t) = \frac{1}{2\pi}\frac{d}{dt}\arctan\left(\frac{\overline{C}_i(t)}{C_i(t)}\right) \tag{4}$$

[29]. Therefore, we construct the pair of functions $[C_i(t), \omega_i(t)]$ for all IMF modes, and this concludes the standard HHT procedure. Let us stress again the fully *adaptive* nature of the HHT: The IMFs are not defined *a priori*, and they accommodate the oscillatory degree of the analyzed signal without postulating systematic "structures" [29,30]. The most important consequence is that the HHT is typically free of subharmonics [23,27,28]. Here, in order to investigate the amplitude of turbulent velocity fluctuations versus their characteristic frequency, we define the ω-dependent q-order statistical moment $\mathcal{L}_q(\omega)$ by computing the moments of each IMF conditioned on those instants of time where the corresponding *instantaneous* frequency has a given value $\omega_i(t) = \omega$,

$$\mathcal{L}_q(\omega) \equiv \sum_{i=1}^{n} \langle |C_i|^q | \omega \rangle_t, \tag{5}$$

where $q \geqslant 0$ is a real number, and with $\langle \cdots \rangle_t$ we denote time and ensemble averaging over different trajectory realizations. We call it the Hilbert spectrum (HS) of order q. Let us notice that each HS can be seen as a superimposition of spectra obtained from different IMFs.

From a dimensional point of view the simplest link between the instantaneous frequency ω and the coherence time of

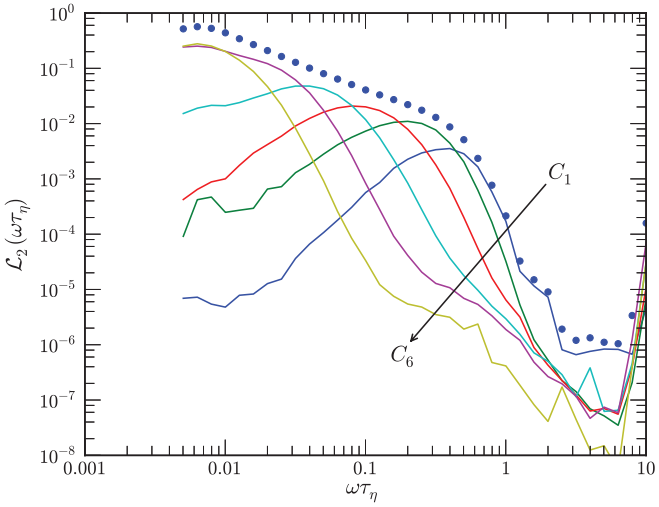

FIG. 2. (Color online) Log-log plot of the second-order Hilbert spectrum, $\mathcal{L}_2(\omega) \equiv \Sigma_{i=1}^{n} \langle |C_i|^2 | \omega \rangle_t$, superimposed with the different contributions from each IMF, $\langle (C_i)^2 | \omega \rangle$ with $i = 1, \ldots, 6$.

an eddy τ is the reciprocal relation $\omega \sim \tau^{-1}$. Therefore, we postulate for the general HS of order q a scaling relation of the form

$$\mathcal{L}_q(\omega) \sim \omega^{-\zeta_L(q)}; \tag{6}$$

here, $\zeta_L(q)$ must be compared with the scaling exponent provided by the LSF [28]. The above scaling relation was validated by using both fractional Brownian motion with various Hurst numbers $0 < H < 1$ for monofractal processes and a lognormal signal with an intermittent parameter $\mu = 0.15$ as an example of a multifractal process. For all cases, the scaling exponents provided by the HHT agree with the ones derived by the standard SF method and with the theoretical ones [28]. To begin with, we focus on the case $q = 2$, that, as mentioned, is related to the amplitude of energy fluctuations as a function of its coherence time or characteristic frequency. In Fig. 2 we show the second-order HS, $\mathcal{L}_2(\omega)$ vs ω in log-log, superimposed with the contributions from each different IMF order. As one can see, only the whole reconstructed HS shows a good scaling behavior. In order to better compare the HS to LSF curves we plot them in Fig. 3 in compensated form in such a way that the expected behavior in the inertial range would be given by a constant, respectively, $S_2(\tau)(\epsilon\tau)^{-1}$ vs τ and $\mathcal{L}_2(\omega)\epsilon^{-1}\omega$ vs $1/\omega$. For completeness, in the same figure, the compensated behavior of the Fourier spectrum, $E(f)\epsilon^{-1}f^2$ vs $1/f$, is also provided. The first striking difference between HS and LSF or Fourier is the enhanced scaling property of the new quantity. We also note that the shape of the LSF curve is consistent with the one in Refs. [8,9], where no plateau was observed in the inertial range. On the compensated scale the Fourier spectrum behaves better than the LSF, but the range of scaling is about half of that of the Hilbert spectrum. Such a difference is even more evident when the logarithmic local slopes are compared (see the inset of Fig. 3). A clear inertial scaling range, $0.01 < \omega\tau_\eta < 0.2$, corresponding to an interval of time scales $5 < \tau/\tau_\eta < 100$, is observed for the compensated $\mathcal{L}_2$. The reason why LSF fails in displaying scaling is that it mixes low (infrared, IR)/high (ultraviolet,

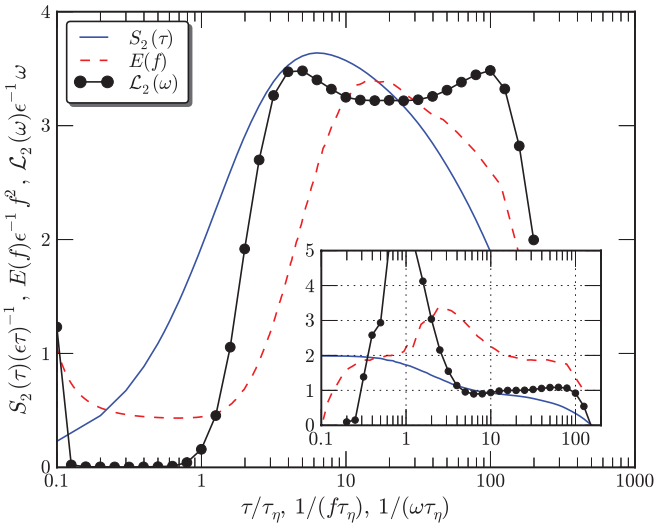

FIG. 3. (Color online) Comparison between the second-order compensated Lagrangian structure function $S_2(\tau)/(\epsilon\tau)$ vs τ/τ_η (solid line), the compensated Fourier spectrum $E(f)/\epsilon^{-1}f^2$ vs $1/(f\tau_\eta)$ (dashed line), and the corresponding Hilbert spectrum $\mathcal{L}_2(\omega)\epsilon^{-1}\omega$ vs $1/(\omega\tau_\eta)$ (•), where τ_η represents the dissipative time scale of the turbulent flow and ϵ the mean energy dissipation rate. Lower inset: The logarithmic local slopes for $d\log S_2(\tau)/d\log\tau$ vs τ/τ_η, $d\log E(f)/d\log f$ vs $1/(f\tau_\eta)$, and $d\log\mathcal{L}_2(\omega)/d\log\omega$ vs $1/(\omega\tau_\eta)$. Note that the expected inertial scaling exponents are, respectively, $S_2(\tau) \sim \tau^{\zeta_L(2)}$, $E(f) \sim f^{-[\zeta_L(2)+1]}$, and $\mathcal{L}_2(\omega) \sim \omega^{-\zeta_L(2)}$, with $\zeta_L(2) = 1$.

UV) frequency fluctuations to the ones in the inertial range $\sim[10^{-2}, 10^{-1}]\tau_\eta^{-1}$. This becomes explicit when considering the relation $S_2(\tau) \propto \int_0^{+\infty} E(f)(1 - \cos 2\pi f\tau)df$, and defining

$$\mathcal{R}_{f_m}^{f_M}(\tau) \equiv S_2(\tau)^{-1} \int_{f_m}^{f_M} E(f')(1 - \cos(2\pi f'\tau))df', \tag{7}$$

which measures the relative contributions to $S_2(\tau)$ from the frequency range $[f_m, f_M]$. When such an interval is set to $[0, 10^{-2}]\tau_\eta^{-1}$ we get the low-frequency contributions, and with $[10^{-1}, +\infty]\tau_\eta^{-1}$ the high ones. In Fig. 4, we show that such spurious nonlocal contributions can be as high as 80%.

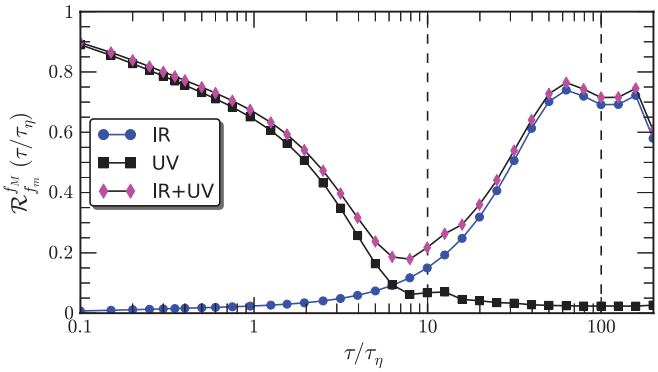

FIG. 4. (Color online) Relative contribution of Fourier frequencies in the range $[f_m, f_M]$ to the $S_2(\tau)$ LSF, as from Eq. (7). Low (IR) frequencies $[0, 10^{-2}]\tau_\eta^{-1}$ and high (UV) frequencies $[10^{-1}, +\infty]\tau_\eta^{-1}$. Vertical lines denote the empirically defined inertial range.

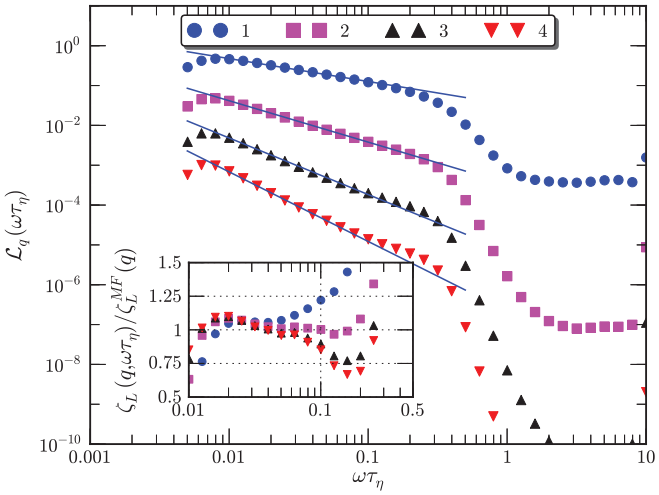

FIG. 5. (Color online) The Hilbert spectra $\mathcal{L}_q(\omega\tau_\eta)$ for $q = 1,2,3,4$. For display clarity, the curves have been vertically shifted by factors 10^{-1}, 10^{-2}, and 10^{-3} for $q = 2$, 3, and 4. Solid lines come from least square fit in the range $0.01 < \omega\tau_\eta < 0.1$. The inset shows the comparison of the measured local scaling exponent $\zeta_L(q,\omega\tau_\eta) = d\log\mathcal{L}_q(\omega)/d\log\omega$ with the multifractal prediction $\zeta_L^{\mathrm{MF}}(q)$.

The HS functions $\mathcal{L}_q(\omega)$ have good scaling properties also for other q orders. We calculated $\mathcal{L}_q(\omega)$ for the orders $q = 1,2,3,4$, and empirically found a good power law behavior in the range $0.01 < \omega\tau_\eta < 0.1$ (respectively $10 < \tau/\tau_\eta < 100$), as shown in Fig. 5. This allows to extract the scaling exponents directly in the instantaneous frequency space, without resorting to the above mentioned ESS procedure. The numerical values for the $\zeta_L(q)$ extracted from the fit in the range $0.01 < \omega\tau_\eta < 0.1$ are reported in Table I. The values of the scaling exponents are estimated as the average of the logarithmic local slope $\zeta_L(q,\omega) = d\log\mathcal{L}_2(\omega)/d\log\omega$ on the above interval and the error bars as the difference between the averages taken on only the first or the second half (in log scale) of the fitted frequency range. Note that the indicated errors are larger than the estimated statistical errors. Here, statistical convergence was checked by performing the same analysis on random subsets with 1/64 of the total data. First, let us notice the evident departure from the dimensional estimate (named K41 [34]), $\zeta_L^{\mathrm{K41}}(q) = q/2$. Second, the measured values are in good agreement with the prediction given by the multifractal model ζ_L^{MF} [12]. In order to better appreciate the quality of our scaling, we show in the inset of Fig. 5 the logarithmic local slope empirically measured with the HHT, $\zeta_L(q,\omega)$, compensated with the predicted value from the multifractal phenomenology, such that a plateau around the value 1 is the indication of the existence of an intermittent multifractal power law behavior.

TABLE I. Lagrangian scaling exponents $\zeta_L(q)$ for orders $q = 1,4$ as estimated from dimensional analysis $q/2$ (K41), from the multifractal model (MF) [12], and as obtained here from Hilbert spectra (HS).

	$q=1$	$q=2$	$q=3$	$q=4$
$\zeta_L^{\mathrm{K41}}(q)$	0.5	1.0	1.5	2.0
$\zeta_L^{\mathrm{MF}}(q)$	0.55	1	1.38	1.71
$\zeta_L^{\mathrm{HS}}(q)$	0.59 ± 0.06	1.03 ± 0.03	1.39 ± 0.10	1.70 ± 0.14

In summary, we have presented a Hilbert-Huang transform-based methodology to capture the intermittent nature of the turbulent Lagrangian velocity fluctuations. Our test bench has been a numerical database of homogeneous isotropic turbulence at $\mathrm{Re}_\lambda = 400$. The first result is that for the second-order statistical moment $\mathcal{L}_2(\omega)$, an energylike quantity, we observe a clear inertial range versus time defined as $\tau = \omega^{-1}$ for at least one decade, in the range $0.01 < \omega\tau_\eta < 0.2$. Such clean scaling can not be highlighted using more standard methods. Second, we extracted the hierarchy of the scaling exponent $\zeta_L(q)$ without applying ESS. Our measurements provide a solid confirmation to the predictions of the multifractal model. The Hilbert method we applied here is general and can be applied to other systems with multiscale dynamics, e.g., Rayleigh-Bénard convection [35], two-dimensional turbulence [36,37].

This work is sponsored by the National Natural Science Foundation of China (Grants No. 11072139, No. 11032007, and No. 11202122), "Pu Jiang" project of Shanghai (No. 12PJ1403500), the Shanghai Program for Innovative Research Team in Universities, COST Action MP0806 "Particles in turbulence," and in part by the Foundation for Fundamental Research on Matter (FOM), which is part of the Netherlands Organization for Scientific Research (NWO). The DNS data used in this study are freely available from the iCFD database [38]. We thank Dr. G. Rilling and Prof. P. Flandrin for sharing their EMD code, which is available at [39].

[1] P. Yeung, Annu. Rev. Fluid Mech. **34**, 115 (2002).
[2] F. Toschi and E. Bodenschatz, Annu. Rev. Fluid Mech. **41**, 375 (2009).
[3] O. Kamps, R. Friedrich, and R. Grauer, Phys. Rev. E **79**, 066301 (2009).
[4] P. K. Yeung, S. B. Pope, and B. L. Sawford, J. Turbul. **7**, 58 (2006).
[5] H. Xu, M. Bourgoin, N. T. Ouellette, and E. Bodenschatz, Phys. Rev. Lett. **96**, 024503 (2006).
[6] N. Mordant, J. Delour, E. Léveque, O. Michel, A. Arnéodo, and J.-F. Pinton, J. Stat. Phys. **113**, 701 (2003).
[7] L. Chevillard, S. G. Roux, E. Leveque, N. Mordant, J. F. Pinton, and A. Arneodo, Phys. Rev. Lett. **95**, 064501 (2005).
[8] B. Sawford and P. Yeung, Phys. Fluids **23**, 091704 (2011).
[9] G. Falkovich *et al.*, Phys. Fluids **24**, 055102 (2012).
[10] M. S. Borgas, Philos. Trans. R. Soc. London A **342**, 379 (1993).
[11] G. Boffetta, F. De Lillo, and S. Musacchio, Phys. Rev. E **66**, 066307 (2002).

[12] L. Biferale, G. Boffetta, A. Celani, B. J. Devenish, A. Lanotte, and F. Toschi, Phys. Rev. Lett. **93**, 064502 (2004).
[13] F. G. Schmitt, Physica A **368**, 377 (2006).
[14] H. Homann, O. Kamps, R. Friedrich, and R. Grauer, New J. Phys. **11**, 073020 (2009).
[15] G. W. He, Phys. Rev. E **83**, 025301 (2011).
[16] L. Biferale, E. Calzavarini, and F. Toschi, Phys. Fluids **23**, 085107 (2011).
[17] A. Arnéodo *et al*., Phys. Rev. Lett. **100**, 254504 (2008).
[18] R. Benzi, S. Ciliberto, R. Tripiccione, C. Baudet, F. Massaioli, and S. Succi, Phys. Rev. E **48**, R29 (1993).
[19] L. Biferale, G. Boffetta, A. Celani, B. Devenish, A. Lanotte, and F. Toschi, Phys. Fluids **17**, 115101 (2005).
[20] X. Zhu, Z. Shen, S. D. Eckermann, M. Bittner, I. Hirota, and J. H. Yee, J. Geophys. Res **102**, 16545 (1997).
[21] S. J. Loutridis, Eng. Struct. **26**, 1833 (2004).
[22] D. A. T. Cummings, R. A. Irizarry, N. E. Huang, T. P. Endy, A. Nisalak, and K. Ungchusak, Nature (London) **427**, 344 (2004).
[23] N. E. Huang, in *Hilbert-Huang Transform and Its Applications* (World Scientific, Singapore, 2005), Chap. 1, pp. 1–26.
[24] Z. H. Wu, N. E. Huang, S. R. Long, and C. K. Peng, Proc. Natl. Acad. Sci. USA **104**, 14889 (2007).
[25] X. Y. Chen, Z. H. Wu, and N. E. Huang, Adv. Adapt. Data Anal. **2**, 233 (2010).
[26] Y. Huang, F. Schmitt, Z. Lu, and Y. Liu, Europhys. Lett. **84**, 40010 (2008).
[27] Y. Huang, F. G. Schmitt, Z. Lu, P. Fougairolles, Y. Gagne, and Y. Liu, Phys. Rev. E **82**, 026319 (2010).
[28] Y. Huang, F. G. Schmitt, J. P. Hermand, Y. Gagne, Z. Lu, and Y. Liu, Phys. Rev. E **84**, 016208 (2011).
[29] N. E. Huang, Z. Shen, S. R. Long, M. C. Wu, H. H. Shih, Q. Zheng, N. Yen, C. C. Tung, and H. H. Liu, Proc. R. Soc. London, Ser. A **454**, 903 (1998).
[30] P. Flandrin and P. Gonçalvès, Int. J. Wavelets, Multires. Info. Process. **2**, 477 (2004).
[31] R. Benzi, L. Biferale, E. Calzavarini, D. Lohse, and F. Toschi, Phys. Rev. E **80**, 066318 (2009).
[32] N. E. Huang, Z. Shen, and S. R. Long, Annu. Rev. Fluid Mech. **31**, 417 (1999).
[33] G. Rilling, P. Flandrin, and P. Gonçalvès, in *Proceedings of the Sixth IEEE-EURASIP Workshop on Nonlinear Signal and Image Processing (NSIP '03) Grado, Italy, 2003* (IEEE, New York, 2003).
[34] A. S. Monin and A. M. Yaglom, *Statistical Fluid Mechanics* (MIT Press, Cambridge, MA, 1971), Vol. II.
[35] D. Lohse and K.-Q. Xia, Annu. Rev. Fluid Mech. **42**, 335 (2010).
[36] G. Boffetta and R. Ecke, Annu. Rev. Fluid Mech **44**, 427 (2012).
[37] F. Bouchet and A. Venaille, Phys. Rep. **515**, 227 (2012).
[38] http://cfd.cineca.it.
[39] G. Rilling and P. Flandrin, http://perso.ens-lyon.fr/patrick.flandrin/emd.html.